Introduction

Attenuation and anisotropy are increasingly indispensable components of wavefield simulation in seismic exploration and monitoring applications. They are especially important in modern seismic amplitude modelling and reverse time migration (RTM) procedures. Anelastic attenuation of the wavefield during propagation due to energy loss, when unaccounted for, reduces image resolution. This amplitude loss can be mitigated through inverse Q processing, wherein an equivalent data set, absent attenuation and dispersion, is estimated (Bickel and Natarajan, 1985; Innanen and Lira, 2010), but these tend to have been developed for simple media and can produce inconsistent results in regions of complex geology. Xu et al. (2015)derive a pure P-wave equation for viscoacoustic TTI media from Christoffels equation and introducing isotropic attenuation with one SLS. Fletcher et al. (2012) introduced amplitude and phase filters to be applied separately to source and receiver wavefields, allowing amplitude and phase effects to be corrected. Dutta and Schuster (2014) employed a least-squares RTM (LSRTM) approach for attenuation compensation based on a standard linear solid (SLS) model and its adjoint operator (Blanch and Symes, 1995) with a simplified stress-strain relation. Zhu and Harris (2014) introduced a constant-Q viscoacoustic wave equation with separate fractional Laplacians and applied it to the problem of Q-compensated RTM (Zhu et al., 2014). Suh et al. (2012) extended the viscoacoustic wave equation for anisotropic media and set out a VTI viscoacoustic reverse time migration algorithm. In this paper, building on the work reported by Fathalian and Innanen (2018), beginning with a SLS model, we formulate a time-domain anisotropic viscoacoustic wave equation. This equation describes constant-Q (Kjartansson, 1979) wave propagation and contains independent terms for phase dispersion and amplitude attenuation, such that through appropriate sign reversal attenuation and dispersion can be individually affected in the modelled wavefield. This TTI viscoacoustic wave equation is used as the basis for a Q-RTM methodology that can corrects for both amplitude attenuation and phase dispersion in the migrated images. The simulated data sets are employed to examine the accuracy of the imaging method. In particular, we demonstrate that the when combined with the cross-correlation imaging condition, Q-RTM compensates for amplitude attenuation and phase dispersion in the receiver wavefields.

Viscoacoustic wave equation in TTI media

We adopt an attenuation model which is linear in frequency (Kjartansson, 1979), implying a frequency-independent Q. The 2D first-order differential TTI viscoacoustic wave equations based on this attenuation model are shown. By selecting the single mechanism, i.e., L = 1, the wave equations can be written as

$$\partial_t \sigma_H = \rho V_P^2 \left[(1+2\varepsilon) \left[\left(\frac{\tau_\varepsilon}{\tau_\sigma} \right) [(\cos\theta \cos\varphi\, \partial_x - \sin\theta\, \partial_z) u_x] + r_H \right] \right] + \sqrt{1+2\delta} [(\cos\varphi \sin\theta\, \partial_x + \cos\theta \partial_z) u_z], \quad (1)$$

$$\partial_t \sigma_V = \rho V_P^2 \left[\sqrt{1+2\delta} [(\cos\theta \cos\varphi\, \partial_x - \sin\theta\, \partial_z) u_x] + \left(\frac{\tau_\varepsilon}{\tau_\sigma} \right) [(\cos\varphi \sin\theta\, \partial_x + \cos\theta \partial_z) u_z] + r_V \right], \quad (2)$$

Where $u_x(X,t)$ and $u_z(X,t)$ are the particle velocity components in the x- and z-directions respectively, σ_H and σ_V are the horizontal and vertical stress components respectively, ρ is the density, r is a memory variable, ε and δ are Thomsen parameters, θ is the tilt angle, and φ is the azimuth of tilt for TTI symmetry axis. The memory variables for horizontal and vertical stress, r_H and r_V (Carcione et al., 1988a), satisfy

$$\partial_t r_H = -\frac{1}{\tau_\sigma} r_H + [(\cos\theta \cos\varphi\, \partial_x - \sin\theta\, \partial_z)] \frac{1}{\tau_\sigma} \left(1 - \frac{\tau_\varepsilon}{\tau_\sigma} \right), \quad (3)$$

$$\partial_t r_V = -\frac{1}{\tau_\sigma} r_V + [(\cos\varphi \sin\theta\, \partial_x + \cos\theta\, \partial_z)] \frac{1}{\tau_\sigma} \left(1 - \frac{\tau_\varepsilon}{\tau_\sigma} \right), \quad (4)$$

The stress and strain relaxation parameters, τ_σ and τ_ε, are related to the quality factor Q and the reference angular frequency ω (Robertsson et al., 1994). In attenuating media, a wave is

undergoing two primary changes, a reduced amplitude and a phase shift due to dispersion. When simulating attenuative wave propagation one may wish to include only the amplitude loss effect, only the phase dispersion effect, or both. In our approach, we will explicitly separate phase dispersion and amplitude attenuation in equations 1 and 2. After some algebraic manipulation and elimination of memory variables, the constant-Q viscoacoustic TTI equations underlying our imaging algorithms can be obtain as

$$\partial_t \sigma_H = \rho V_P^2 \left[(1+2\varepsilon) \left[\left(a_1 \frac{2}{A} + i a_2 \frac{2}{AQ} \right) [(\cos\theta \cos\varphi\, \partial_x - \sin\theta\, \partial_z) u_x] \right] \right.$$
$$\left. + \sqrt{1+2\delta} [(\cos\varphi \sin\theta\, \partial_x + \cos\theta \partial_z) u_z] \right] \quad (5)$$

$$\partial_t \sigma_V = \rho V_P^2 \left[\sqrt{1+2\delta} [(\cos\theta \cos\varphi\, \partial_x - \sin\theta\, \partial_z) u_x] + \left(a_1 \tfrac{2}{A} + i a_2 \tfrac{2}{AQ} \right) [(\cos\varphi \sin\theta\, \partial_x + \cos\theta \partial_z) u_z] \right], \quad (6)$$

Where $A = 1 + \left(\sqrt{1 + 1/Q^2} - 1/Q \right)^2$ within the dispersion-dominated and attenuation dominated operators 2/A and 2/AQ (respectively). The coefficients a_1 and a_2, which can take on values of +1, 0 or -1, have been formally introduced to permit inclusion, suppression and/or reversal of the processes of attenuation and dispersion. In the acoustic limit $Q \to \infty$, the dispersion-dominated operator lapses to 1 and the attenuation-dominated vanishes. To illustrate the decoupling of velocity dispersion and amplitude losses in numerical simulations based on these equations, we consider a homogeneous model with a background velocity of 2500 m/s and quality factor Q=10. The Thomsen parameters are set to ε = 0.2 and δ = 0.05, and the symmetry axis is tilted at 45°. In the four panels of Figure 1 the top right corner of the model is plotted with a snapshot of the compressional P wavefront overlain. The wavefront is approximately ellipsoidal. A snapshot of a reference (acoustic) wavefield is plotted in Figure 1a. The dashed yellow line touches the leading edge of the reference wavefront. The amplitude-loss simulation (a_1= 0 and a_2= 1) is plotted in Figure 1b. Compared with the acoustic case, the amplitude is attenuated, but the phases are the same. The phase dispersion simulation (a_1= 1 and a_2= 0) is plotted in Figure 1c. The phase has a delay, and the amplitude is similar to the acoustic case. In Figure 1d the viscoacoustic wavefield calculated with equations 5 and 6 is plotted. The reduced amplitude and phase delay (relative to the acoustic reference wavefield) are visible.

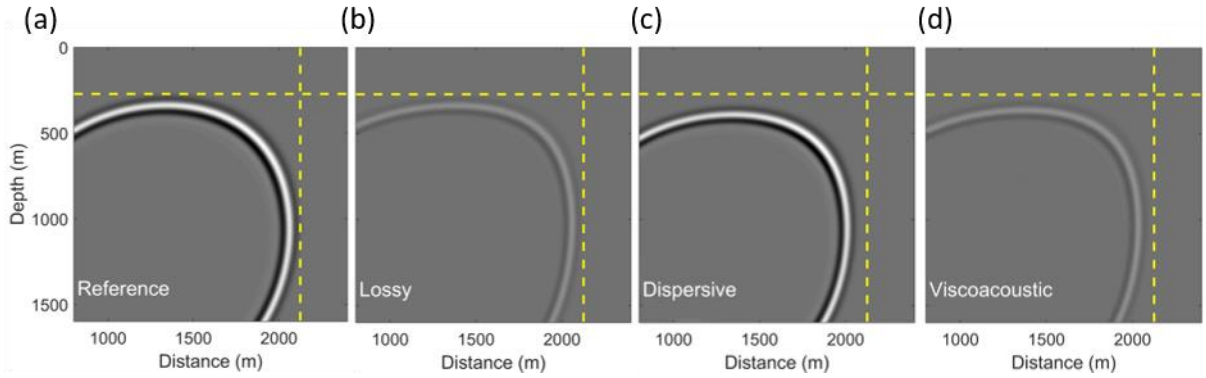

Figure 1 *2D wavefield snapshots in TTI media using (a) acoustic, (b) amplitude loss, (c) dispersive, and (d) viscoacoustic data with ε = 0.2, δ = 0.05, and θ=45.*

In RTM, a receiver wavefield is reversed in time, and then propagated through the velocity model to each image point. The act of forward propagation of a time-reversed field, which undoes all (but only) time-reversible phenomena of wave propagation, leads to the requirement for special treatment of attenuation. With attenuation and dispersion separated in the viscoacoustic equations, this issue can be easily addressed. The sign of a_2 controls attenuation. To arrange for amplitude compensation, we reverse its sign, i.e., set a_2 = -1. Conversely, for correction of dispersion the sign of the associated coefficient remains unchanged: a_1 = 1. The main concern during compensating for attenuation effects is the possible amplification of unwanted frequencies in data because the recorded data are often infected with high-frequency noise. To avoid high-frequency noise from growing exponentially, we

apply a low-pass filter in the wavenumber domain. The cutoff wavenumber is calculated by the cutoff frequency over the maximum velocity of the model. A suitable cutoff frequency is determined by identifying a value based on the noise level of spectrum of the observed data.

Numerical examples

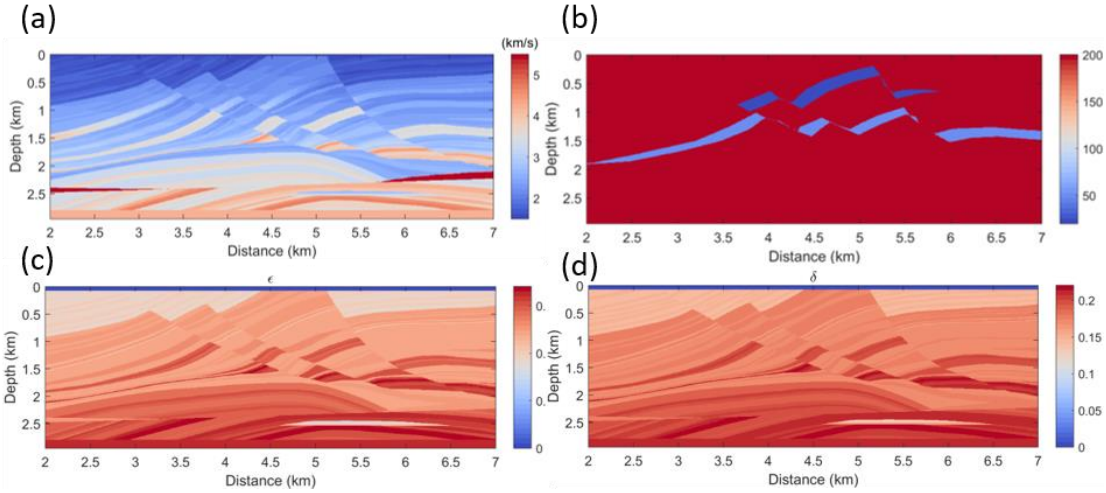

Figure 2 *The Marmousi models: (a) true velocity model, (b) true Q model, (c) Thomsen's ε model model, and (d) Thomsen's δ model.*

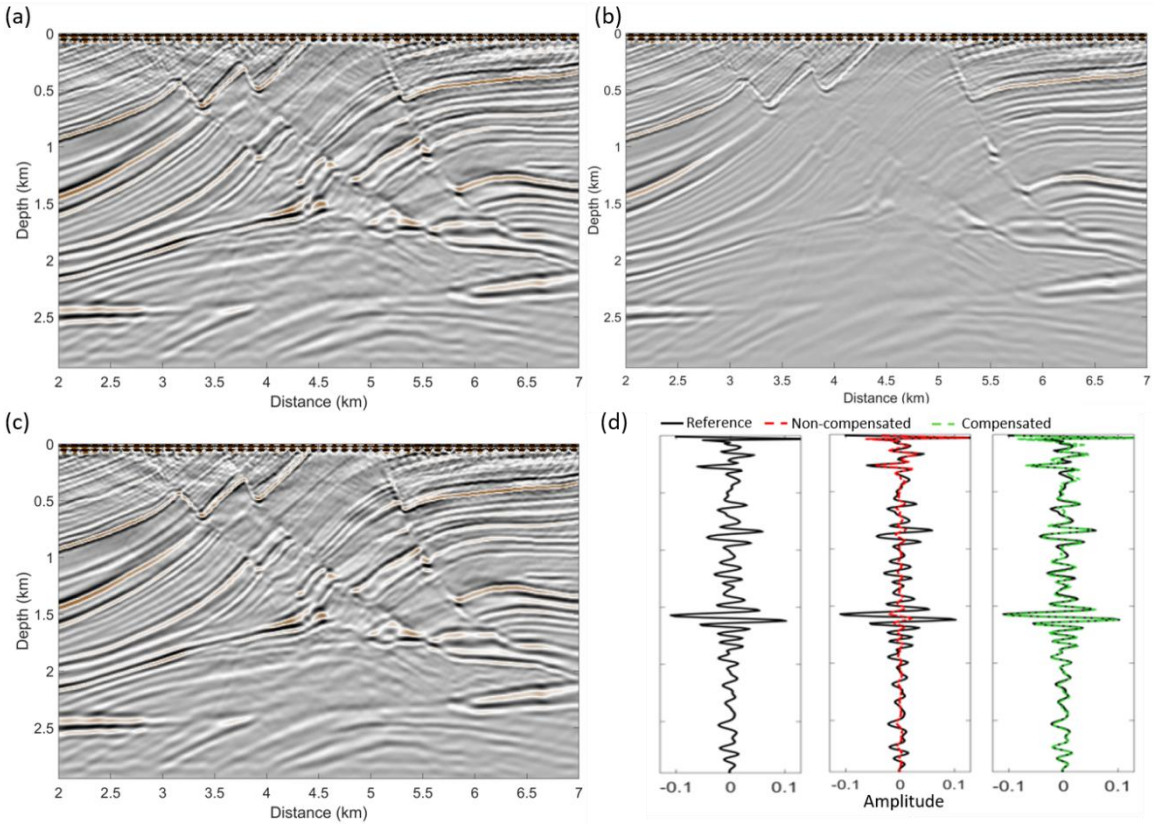

Figure 3 *Comparison among from (a) acoustic RTM (reference), (b) acoustic RTM with viscoacoustic data, (c) Q-RTM with viscoacoustic data, and (d) show the reference trace (blue line), non-compensated trace (red line), and compensated trace (dashed green line)at the horizontal 4.2 km. The compensated case agree with the reference image very well.*

We examine the numerical response of this approach to TTI Q-RTM, with an augmented Marmousi model. In Figure 2 the actual velocity model, the corresponding true Q model, and the associated Thomsen parameter models are plotted. We produce a synthetic viscoacoustic TTI data set by setting

the tilt angle to 45°. As before, shear wave artifacts are avoided by setting up small smoothly tapered circular regions with $\varepsilon = \delta$ around the source positions (Duveneck et al., 2008). The model grid dimensions are 281×701 , and the grid size is 10×10 m. Sources and receivers are positioned along the surface at a depth of 30 m, and a zero-phase Ricker wavelet with 15 Hz center frequency is adopted. The sampling interval rate is 0.4 ms, and the recording length is 3 s. The reference RTM image (Figure 3a) has similar amplitudes in the shallower layers, when compared with the non-compensated RTM image, but in the non-compensated case (Figure 3b) weak amplitudes in the deeper layers, especially beneath the layers with strong attenuation, are evident. The compensated RTM image (Figure 3c) has recovered reflector amplitudes at the dipping deeper layers, for which the image amplitudes compare well with those of the reference case. To verify that the reflectors have been migrated to the correct positions, we include image profiles from a fixed lateral position in Figure 3d. The non-compensated trace (dashed red line) has a shifted phase and a reduced amplitude. The compensated traces (dashed green line) have amplitude and phase comparable to the reference case (solid black line). We view these examples as evidence that the proposed Q-RTM approach in TTI media are well-posed and generate well-resolved and artifact-free images when both anisotropic and viscous processes are active for a surface data set.

Conclusions

We have presented a time-domain viscoacoustic RTM imaging algorithm in tilted TI media based on a series of standard linear solid mechanisms, which mitigates attenuation and dispersion effects in migrated images. The wave equations have been extended from isotropic media to tilted TI media. The amplitude loss and phase dispersion in the source and receivers wavefields can be recovered by applying compensation operators on the measured receiver wavefield. The phase dispersion and amplitude attenuation operators in Q-RTM approach are separated, and the compensation operators are constructed by reversing the sign of the attenuation operator without changing the sign of the dispersion operator. With sufficiently accurate Q and velocity models, the TTI Q-RTM can produce better images than isotropic RTM, especially in areas with anisotropy, attenuation and strong variations of dip angle. Numerical tests on synthetic data illustrate also that this approach can improve the image resolution beneath areas with strong attenuation.

References

Bickel, S. and Natarajan, R. [1985] Plane-wave Q deconvolution. *Geophysics*, **50**, 1426-1439.
Blanch, J.O. and Symes, W.W. [1995] Efficient iterative viscoacoustic linearized inversion. *65th Annual International Meeting*, SEG, Expanded Abstracts, 627-630.
Dutta, G. and Schuster, G.T. [2014] Attenuation compensation for least-squares reverse time migration using the viscoacoustic-wave equation. *Geophysics*, **79**, S251-S262.
Duveneck, X., Fletcher, R.P. and Fowler, P.J. [2008] A new pseudo-acoustic wave equation for VTI medium. *70th EAGE Conference & Exhibition*, Extended Abstracts, H033.
Fathalian, A. and Innanen, K.A. [2018] Viscoacoustic VTI and TTI wave equations applied in constant-Q anisotropic reverse time migration. *88th Annual International Meeting*, SEG, Expanded Abstracts 241-245.
Fletcher, R., Nichols, D. and Cavalca, M. [2012] Wavepath-consistent effective Q estimation for Q-compensated reverse-time migration. *74th EAGE Conference & Exhibition*, Extended Abstracts.
Innanen, K.A. and Lira, J.E. [2010] Direct nonlinear Q-compensation of seismic primaries reflecting from a stratified, two-parameter absorptive medium. *Geophysics*, **75**, V13-V23.
Kjartansson, E. [1979] Constant Q-wave propagation and attenuation: Journal of Geophysical Research. *Solid Earth*, **84**, 4737-4748.
Suh, S., Yoon, K., Cai, J. and Wang, B. [2012] Compensating viscoacoustic effects in anisotropic resverse-time migration. *82nd Annual International Meeting*, SEG, Expanded Abstracts, 1-5.
Xu, W., Yang, G., Li, H. and Wang, J. [2015] Pure viscoacoustic equation of TTI media and applied it in anisotropic RTM. *85th Annual International Meeting*, SEG, Expanded Abstracts, 525-529.
Zhu, T. and Harris, J.M. [2014] Modeling acoustic wave propagation in heterogeneous attenuating media using decoupled fractional laplacians. *Geophysics*, **79**, T105-T116.